Pattern Recognition 93 (2019) 14–24

Contents lists available at ScienceDirect

Pattern Recognition

journal homepage: www.elsevier.com/locate/patcog

Correntropy based scale ICP algorithm for robust point set registration

Zongze Wu[a], Hongchen Chen[b], Shaoyi Du[c,*], Minyue Fu[a], Nan Zhou[d], Nanning Zheng[c], Fellow, IEEE

[a] School of Automation, Guangdong University of Technology, Guangzhou 510006, China
[b] School of Electronic and Information, South China University of Technology, Guangzhou 510640, China
[c] Institute of Artificial Intelligence and Robotics, Xi'an Jiaotong University, Xi'an 710049, China
[d] School of Automation Engineering, University of Electronic Science and Technology of China, Chengdu 611731, China

ARTICLE INFO

Article history:
Received 16 February 2017
Revised 22 June 2017
Accepted 19 March 2019
Available online 30 March 2019

Keywords:
Iterative closest point
Correntropy
Scale transformation
Point set registration
Outliers

ABSTRACT

The iterative closest point (ICP) algorithm has the advantage of high accuracy and fast speed for point set registration, but it performs poorly when the point sets have a large number of outliers and noises. To solve this problem, in this paper, a novel robust scale ICP algorithm is proposed by introducing maximum correntropy criterion (MCC) as the similarity measure. As the correntropy has the property of eliminating the interference of outliers and noises compared to the commonly used Euclidean distance, we use it to build a new model for scale registration problem and propose the robust scale ICP algorithm. Similar to the traditional ICP algorithm, this algorithm computes the index mapping of the correspondence and a transformation matrix alternatively, but we restrict the transformation matrix to include only rotation, translation and a scale factor. We show that our algorithm converges monotonously to a local maximum for any given initial parameters. Experiments on synthetic and real datasets demonstrate that the proposed algorithm greatly outperforms state-of-the-art methods in terms of matching accuracy and run-time, especially when the data contain severe outliers.

1. Introduction

As a fundamental technique in computer vision, pattern recognition and image analysis, image registration [1,2] has been an increasingly important research topic. Many tasks in image registration, such as medical image registration [3,4], can be formulated as matching two sets of feature points, more specifically, as a point set registration problem. The feature points are typically the edge points sampled from a shape contour or the locations of sparse points extracted from an image. The goal of point set registration is to determine the correct correspondence and recover the underlying transformation between two point sets.

In general, point set registration can be separated into two subtasks: (1) establish the index matching between two point sets, and (2) find the spatial transformation that aligns the two point sets. It is easy to solve each of these subtasks once the solution to the other is known. Nevertheless, it is much more difficult and challenging to solve both of them concurrently. Thus, many researchers have devoted great efforts to solve this problem in the past few decades.

One of the best known point set registration approaches is the iterative closest point (ICP) algorithm proposed by Besl and McKay in [5–7]. At each iterative step, the algorithm utilizes the nearest-neighbor relationships to assign a binary correspondence and then compute the spatial transformation based on the current correspondence. The method solves the correspondence and transformation alternatively until it reaches a local minimum. Once a proper initial value is given, the ICP algorithm can perform well in rigid registration. However, it deteriorates quickly in the presence of non-Gaussian noises and cannot complete non-rigid registration.

In practice, the scale factor exists universally in registration. For example, the range data set usually has different scanning resolutions determined by the distances from the sensor to the object surfaces. And images acquired by real digitizers differ greatly in viewpoints. This requires that the registration algorithms be able to estimate the scale parameter, as well as the rotation and translation parameters between images. To deal with the scale registration problem, the original ICP algorithm was extended to scale ICP algorithm where the scale factor is taken into account. By using extended signature images (ESIs) to establish index matching between two image objects even though they are different in scale, Zha et al. [8] thus estimated the scale with this index

* Corresponding author.
E-mail addresses: zzwu@gdut.edu.cn (Z. Wu), dushaoyi@gmail.com (S. Du), minyue.fu@newcastle.edu.au (M. Fu), nnzheng@mail.xjtu.edu.cn (N. Zheng).

https://doi.org/10.1016/j.patcog.2019.03.013
0031-3203/

matching and applied it to traditional ICP for registration. Consider it is time-consuming, Ying et al. proposed the scale ICP algorithm which integrates the scale factor directly into the least squares (LS) problem [9].

It should be pointed out that the above-mentioned approaches can not handle the point sets with a large number of outliers and noises which exist widely in most applications. For example, it is always difficult to extract the contour of an object in most real world applications and the acquired data may have different precisions and random noise due to the precision of the acquisition equipment. To solve such a complex point set registration problem, some scholars used thresholds [10,11] or probability of distance to discard outliers [12–15], but these methods need an appropriate threshold which depends on the structure of point sets and thus is hard to choose. Another approach attempts to reject outliers by adopting a coarse to fine process [16], but the methods often perform poorly in the case of a large number of outliers in the point sets. In addition, the geometrical method [17–19] is used to eliminate noise and outliers, but this would require additional information of the point sets.

Different from the work mentioned above, in this paper, we use correntropy [20–23] to substitute the mean square error (MSE) as the new similarity measure to improve the accuracy and robustness of traditional scale ICP algorithm. Correntropy, which is proposed recently, is directly related to the probability of how similar two random variables are in the joint space controlled by the kernel bandwidth, and yields solutions that are robust to non-Gaussian or impulsive noise. Firstly, we formulate the scale registration problem into an equality constraint optimization problem by applying the maximum correntropy criterion (MCC) [24–28]. To solve such an optimization problem, we imitate the process of ICP and design a fast and accurate iterative procedure based on the half-square technique [24] and singular value decomposition (SVD) method [15]. We also give several comparative experiments to verify that the proposed algorithm is very fast and robust for scale registration with noisy point sets.

The rest of this paper is organized as follows. In Section 2, the definition of correntropy is introduced and the difference between the MSE and the MCC is analyzed. In Section 3, an optimization problem based on the correntropy is derived, and a new scale ICP algorithm is given to solve the optimization problem. Following that is Section 4 in which the proposed technique is evaluated on the experiments and a conclusion is finally drawn in Section 5.

2. Maximum correntropy criterion

净增长

Recently, the concept of correntropy was proposed for information theoretic learning (ITL). It is derived from the generalized correlation function of random processes and is directly related to the information potential (IP) of Renyi's quadratic entropy in which Parzen windowing method is used to estimate the data's probability distribution. Similar to MSE, the correntropy can be a generalized similarity measure between two arbitrary random variables. Here, we firstly introduce the definition of correntropy briefly and present some of its most important properties. After that, we will have a comparison between MSE and correntropy and point out their differences to demonstrate the superiority of correntropy.

2.1. Definition and properties of correntropy

A general form of correntropy between two arbitrary scalar random variables A and B is defined as follows:

$$V_\sigma(A,B) = \mathrm{E}[\kappa_\sigma(A-B)] \tag{1}$$

where $\kappa_\sigma(.)$ is a symmetric positive definite kernel with the kernel width being σ and E(.) denotes the mathematical expectation. The kernel bandwidth controls the "window" in which similarity is assessed and the kernel function maps the input space to a higher dimensional space which has much advantages.

For simplicity, the Gaussian Kernel following is the only one considered in the paper.

$$\kappa_\sigma(A-B) = \frac{1}{\sqrt{2\pi}\sigma}\exp\left(-\frac{(A-B)^2}{2\sigma^2}\right) \tag{2}$$

In practice, the joint probability density function is often unknown and only a finite number of data $\{(a_i,b_i)\}_{i=1}^N$ are available, leading to the sample estimator of correntropy as follows.

$$\hat{V}_{N,\sigma}(A,B) = \frac{1}{N}\sum_{i=1}^{N}\frac{1}{\sqrt{2\pi}\sigma}\exp\left(-\frac{(a_i-b_i)^2}{2\sigma^2}\right) \tag{3}$$

The maximum of correntropy of the error in (3) is called the maximum correntropy criterion.

Next, we present two important properties which will be used later in this paper.

Property 1. *Correntropy is positive definite and bounded, that is,* $0 < V_\sigma(A,B) \le \frac{1}{\sqrt{2\pi}\sigma}$. *It reaches its maximum if and only if* $A = B$.

Property 2. *Correntropy involves all the even moments of the difference between A and B:*

$$V_\sigma(A,B) = \frac{1}{\sqrt{2\pi}\sigma}\sum_{n=0}^{\infty}(-1)^n/(2^n n!)\mathrm{E}[(A-B)^{2n}/\sigma^{2n}] \tag{4}$$

The properties above have already been mentioned and proved in Ref. [20].

2.2. Comparison between MSE and correntropy

The MSE is probably the most widely utilized methodologies for quantifying how similar two random variables are and we know its expression is

$$\mathrm{MSE}(A,B) = \mathrm{E}[(A-B)^2]. \tag{5}$$

In order to make comparison between MSE and correntropy more intuitive, the cost function of them in the joint space of variables A and B are displayed in Fig. 1.

We can easily find that MSE is a quadratic function with a valley along the $a = b$ line. Fig. 1(a) intuitively explains the behavior of MSE in the joint space where for the values away from the $a = b$ line, it takes values that increase quadratically due to the second order moment. The quadratic increase for large error has a net effect of amplifying the contribution of samples that are far away from the mean value of error distribution and it is why MSE works well for data with rapid-decay distributions such as Gaussian. Meanwhile, it is also the reason why other data distributions will make the MSE nonoptimal, especially if the error distribution has big outliers.

MSE includes all the samples in the input space to estimate the similarity of two random variables while correntropy is mainly determined by kernel function along $a = b$ line as Fig. 1(b) shows. That is to say, MSE is global whereas correntropy is local. It shows that correntropy can be used as a new cost function, which is called the maximum correntropy criterion. And because of the locality of correntropy, it has great advantages in non-Gaussian and nonlinear signal processing as a similarity measure, in particular if the error distribution has large outliers.

In order to further understand the correntropy, using a Taylor series expansion of the exponential function in the Gaussian kernel as (4) shows in Property 2. As we can see, correntropy can be viewed as a generalized correlation function between two random variables, including second and higher order moments of the error between them. Therefore, we can know that correntropy

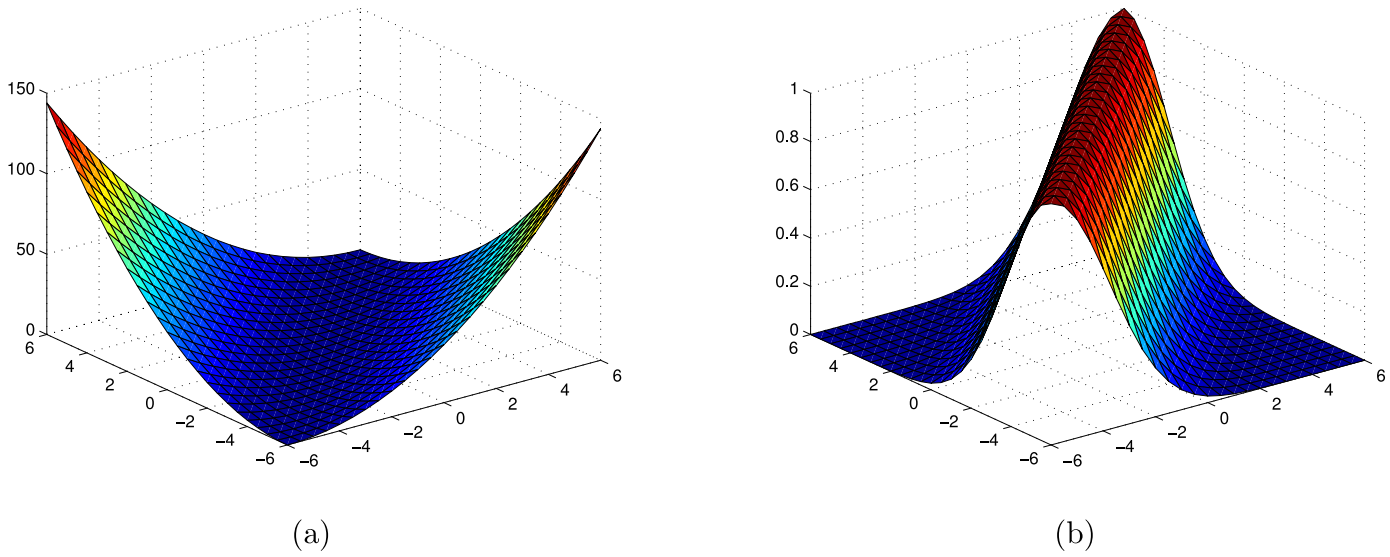

Fig. 1. The distance in the joint space of variables *A* and *B*. (a) Mean square distance. (b) Correntropy.

also quantifies higher order moment of the probability distribution function (PDF) within a small neighborhood determined by the kernel width, which reflects its great advantage in processing signals with impulsive noise and outliers, especially comparing to second order measures.

Furthermore, correntropy has a close relationship with m-estimators, which is a generalized maximum likelihood method performing well in impulsive environments. However, there is no threshold in correntropy and its properties are all controlled by kernel size.

Through the analyses above, we conclude that MCC is a useful measure to handle nonzero mean and non-Gaussian noise with large outliers. We now describe how correntropy can be used as a similarity measure in scale registration to eliminate the effect of outliers.

3. Robust scale ICP algorithm based on correntropy

In this paper, we introduce correntropy and use MCC as similarity measure between two point sets to build a new objective function for scale registration problem. This new algorithm is robust to noises and outliers due to the outlier-reject property of correntropy, which is called robust scale ICP algorithm in this paper. Similar to the traditional scale ICP algorithm, we integrate the scale estimation into the iterative process so that rotation, translation and scale factor are estimated simultaneously in every iteration.

3.1. Scale registration problem

The scale registration of m-D point sets is a difficult problem. To solve this, a general statement is first described as follows.

Given two point sets in $\mathbb{R}^m$, one denotes a model shape $\mathrm{X} \triangleq \{\vec{x}_i\}_{i=1}^{N_x}$ and the other is a data shape $\mathrm{Y} \triangleq \{\vec{y}_i\}_{i=1}^{N_y}$. The registration between two m-D point sets is to find the spatial transformation T, with which X is in the best alignment with Y. To solve this problem, we firstly define an index mapping C: $j = c(i); j \in 1, 2, \ldots, N_y$ which indicates the matching point pairs $\{\vec{x}_i, \vec{y}_{c(i)}\}_{i=1}^{N_x}$. Then, we find the existing scale transformation between X and Y based on the known point pairs. Moreover, the scale transformation consists of a rotation, a translation and a scale factor. We know that the rotation transformation is an orthogonal transformation (i.e.,$\mathbf{R^T R = I}$) with its determinant is 1. Therefore, our robust scale ICP problem is now formulated based on the maximum correntropy criterion as follows:

$$\begin{aligned} &\max_{s,\mathbf{R},\vec{t},c(i)\in\{1,2,\ldots,N_y\}} \sum_{i=1}^{N_x} \exp(-||(s\mathbf{R}\vec{x}_i + \vec{t}) - \vec{y}_{c(i)}||_2^2/(2\sigma^2)) \\ &s.t. \qquad \mathbf{R}^T\mathbf{R} = \mathbf{I}_m,\ \det(\mathbf{R}) = 1 \end{aligned} \tag{6}$$

where s is a scalar scale factor, $\mathbf{R} \in \mathbb{R}^{m\times m}$ is a rotation matrix and $\vec{t} \in \mathbb{R}^m$ is a translation vector. $\vec{y}_{c(i)}$ is the corresponding point of $\vec{x}_i$.

Finally, the scale registration problem can be expressed as an optimization problem for the objective function (6) when correntropy is used to measure.

3.2. Robust scale ICP algorithm

Actually, we can solve this problem in the similar way as the ICP algorithm by iteration. In each iteration, index matching is set up by searching the point in data point set which is the closest to that of the model point set first; then, a scale transformation is computed based on the current index matching. The main two steps of scale ICP algorithm are detailed as follows.

Step 1: Establish the index matching $\{\vec{x}_i, \vec{y}_{c_k(i)}\}$ for these two point sets based on the scale transformation $(s_{k-1}, \mathbf{R}_{k-1}, \vec{t}_{k-1})$ in the previous iteration by maximizing the objective function (6). Actually, it is equivalent to find the closest point in Y for every point in X as the first step of the traditional ICP algorithm.

$$\begin{aligned} c_k(i) = &\arg\min_{c_k(i)\in\{1,2,\ldots,N_y\}} ||(s\mathbf{R}_{k-1}\vec{x}_i + \vec{t}_{k-1}) - \vec{y}_{c_k(i)}||_2^2 \\ &for\ i = 1, \ldots, N_x \end{aligned} \tag{7}$$

Step 2: Compute the transformation $(s_k, \mathbf{R}_k, \vec{t}_k)$ based on the current index matching $\{\vec{x}_i, \vec{y}_{c_k(i)}\}_{i=1}^{N_x}$.

$$(s_k, \mathbf{R}_k, \vec{t}_k) = \arg\max_{\mathbf{R}^T\mathbf{R}=\mathbf{I}_m, \det(\mathbf{R})=1, s, \vec{t}} \sum_{i=1}^{N_x} \exp\left(-\frac{||(s\mathbf{R}\vec{x}_i+\vec{t}) - y_{c_k(i)}||_2^2}{2\sigma^2}\right) \tag{8}$$

The iterations continue until one of the following two conditions is satisfied:

1. $\sum_{i=1}^{N_x} ||(s_k\mathbf{R}_k\vec{x}_i + \vec{t}_k) - \vec{y}_{c_k(i)}||_2^2 \le \varepsilon$, where ε is a sufficiently small positive number.
2. A maximum number of iterations is reached.

Step 1 can be easily solved by many methods such as k-d tree [29] and the nearest point search based on Delaunay tessellation [30]. Studies shows that k-d tree is more applicable

to high-dimensional data while the nearest point search based on Delaunay tessellation is more efficient for two-dimensional or three-dimensional data. Therefore, step 2 of computing the new scale transformation becomes the key for implementing the algorithm. In the following we will solve this difficult problem.

3.3. Computation of transformation

Consider the independence of translation, we can first take the derivative of the objective function $F(s,R,\vec{t})$ with respect to $\vec{t}$ to eliminate the translation transformation.

$$\frac{\partial F}{\partial \vec{t}} = \sum_{i=1}^{N_x}\left(-\frac{s\mathbf{R}\vec{x}_i+\vec{t}-\vec{y}_{c_k(i)}}{\sigma^2}\exp(-||(s\mathbf{R}\vec{x}_i+\vec{t})-y_{c_k(i)}||_2^2/(2\sigma^2))\right) \tag{9}$$

In (9), we use $(s_{k-1},\mathbf{R}_{k-1},\vec{t}_{k-1})$ to substitute $(s_k,\mathbf{R}_k,\vec{t}_k)$ in exponential term and treat it as the weight, which denotes w_i. Because it is quite close between the current transformation and previous transformation, we can do such a approximation and it will not affect the final result. Then we can obtain

$$\vec{t} = \sum_{i=1}^{N_x}(\vec{y}_{c_k(i)} - s\mathbf{R}\vec{x}_i)w_i / \sum_{i=1}^{N_x} w_i. \tag{10}$$

Let $\vec{p}_i \triangleq \vec{x}_i - \sum_{i=1}^{N_x}\vec{x}_i w_i / \sum_{i=1}^{N_x} w_i$, $\vec{q}_i \triangleq y_{c_k(i)} - \sum_{i=1}^{N_x}\vec{y}_{c_k(i)}w_i / \sum_{i=1}^{N_x} w_i$. Therefore,

$$F(s,\mathbf{R}) = \sum_{i=1}^{N_x}\exp(-||s\mathbf{R}\vec{p}_i - \vec{q}_i||_2^2/(2\sigma^2)) \tag{11}$$

To maximize (11), we can recover the following partial differential equations to compute scale and rotation transformation:

$$\frac{\partial F(s,\mathbf{R})}{\partial \mathbf{R}} = \mathbf{0} \tag{12}$$

$$\frac{\partial F(s,\mathbf{R})}{\partial s} = 0 \tag{13}$$

3.3.1. Rotation computation

In ITL, the half-quadratic technique [31–34] is a good method to solve nonlinear ITL optimization problem. Based on the theory of convex conjugated functions [34], we can easily derive the following proposition.

Proposition 1. *Suppose* $g(x) \triangleq \exp(-x^2/2\sigma^2)$, *there exists a convex conjugated function* φ *of* $g(x)$ *such that*

$$g(x) = \max_{u'}\left(u'\frac{\|x\|^2}{\sigma^2} - \varphi(u')\right) \tag{14}$$

where u' *is a scalar variable, and for a fixed x, the maximum is reached at* $u' = -g(x)$ *[25,32].*

Let $x = s\mathbf{R}\vec{p}_i - \vec{q}_i$, *we have the augmented objective function in an enlarged parameter space*

$$\hat{F}(\mathbf{R},\vec{u}) = \sum_{i=1}^{N_x}\left(u_i||s\mathbf{R}\vec{p}_i - \vec{q}_i||_2^2/\sigma^2 - \varphi(u_i)\right) \tag{15}$$

where $\vec{u}=[u_1,\ldots,u_{N_x}]^T$ *is storing the auxiliary variables introduced in the Half-Quadratic optimization.*

$$u_i = -\exp\left(-||s\mathbf{R}\vec{p}_i - \vec{q}_i||_2^2/\left(2\sigma^2\right)\right) \tag{16}$$

In each iteration, we can use the previous scale and rotation to acquire the value of u_i.

Expanding (15), we get

$$\hat{F}(\mathbf{R},\vec{u}) = \sum_{i=1}^{N_x}\left(u_i\left(s^2\vec{p}_i^T\vec{p}_i - 2s\vec{q}_i^T\mathbf{R}\vec{p}_i + \vec{q}_i^T\vec{q}_i\right)/\sigma^2 - \varphi(u_i)\right) \tag{17}$$

Therefore, maximizing $F(\mathbf{R})$ *is equivalent to maximizing the following function.*

$$\begin{aligned} F(\mathbf{R}) &= -\frac{1}{\sigma^2}\sum_{i=1}^{N_x}(u_i s\vec{q}_i^T\mathbf{R}\vec{p}_i) \\ &= -\frac{1}{\sigma^2}tr(u_i\mathbf{R}\vec{p}\vec{q}_i^T) = -tr(\mathbf{RH}) \end{aligned} \tag{18}$$

where $\mathbf{H} = \frac{1}{\sigma^2}\sum_{i=1}^{N_x}u_i\vec{p}_i\vec{q}_i^T$, $tr(.)$ *stands for trace of matrix.*

As a result, for any given s, maximizing $F(s,\mathbf{R})$ *is equivalent to maximizing* $F(\mathbf{R})$ *as (18) shown. We solve it similar to what Du has proposed [15]. But there are something different for the choose of parameter* $\mathbf{D}$, *so we show the derivation process here.*

Let the SVD of $\mathbf{H}$ *be:*

$$\mathbf{H} = \mathbf{U}\mathbf{\Lambda}\mathbf{V} \tag{19}$$

where $\mathbf{U}$ *and* $\mathbf{V}$ *are orthonormal matrices, and* $\mathbf{\Lambda}$ *is a* 3×3 *diagonal matrix with eigenvalues which are ordered from largest to smallest and all nonnegative.*

Considering the objective function with equality constraint items, we use Lagrange multiplier method to solve (18). We define the Lagrange function as follow:

$$L(\mathbf{R},\mathbf{K},\eta) = -tr(\mathbf{RH}) + tr(\mathbf{K}(\mathbf{R}^T\mathbf{R}-\mathbf{I}_n)) + \eta(\det(\mathbf{R})-1) \tag{20}$$

where $\mathbf{K}$ *is a Lagrange multiplier which is a* $m\times m$ *symmetrical matrix,* η *is a Lagrange multiplier and a scalar.*

Taking the derivative with respect to $\mathbf{R}$, $\mathbf{K}$ *and,* η *we obtain*

$$\frac{\partial L}{\partial \mathbf{R}} = -\mathbf{H}^T + 2\mathbf{R}\mathbf{K} + \eta\mathbf{R} = \mathbf{0} \tag{21}$$

$$\frac{\partial L}{\partial \mathbf{K}} = \mathbf{R}^T\mathbf{R} - \mathbf{I}_n = \mathbf{0} \tag{22}$$

$$\frac{\partial L}{\partial \eta} = \det(\mathbf{R}) - 1 = 0 \tag{23}$$

Let $\mathbf{L}' = 2\mathbf{K} + \eta\mathbf{I}$. *From (21), we obtain*

$$\mathbf{R}\mathbf{L}' = \mathbf{H}^T \tag{24}$$

Transpose (24),

$$\mathbf{L}'^T\mathbf{R}^T = \mathbf{H} \tag{25}$$

Multiplying (24) with (25) on both sides, and because $\mathbf{R}^T\mathbf{R} = \mathbf{I}_m$, *we get*

$$\mathbf{L}'^2 = \mathbf{H}\mathbf{H}^T = \mathbf{U}\mathbf{\Lambda}\mathbf{V}^T\mathbf{V}\mathbf{\Lambda}\mathbf{U}^T = \mathbf{U}\mathbf{V}^2\mathbf{U} \tag{26}$$

Obviously, $\mathbf{L}'$ *and* $\mathbf{L}'^2$ *is commutative, that is* $\mathbf{L}'^2\mathbf{L}' = \mathbf{L}'\mathbf{L}'^2$, *so we can use the same orthogonal matrices to simplify it into the form of diagonal matrix.*

$$\mathbf{L}' = \mathbf{U}\mathbf{\Lambda}\mathbf{D}\mathbf{U}^T \tag{27}$$

where $\mathbf{D}=\mathrm{diag}(d_i)$ *is a diagonal matrix with* d_i *is 1 or -1.*

From (27), we know

$$\det(\mathbf{L}') = \det(\mathbf{U}\mathbf{\Lambda}\mathbf{D}\mathbf{U}^T) = \det(\mathbf{\Lambda})\det(\mathbf{D}) \tag{28}$$

From (24), we know

$$\det(\mathbf{L}') = \det(\mathbf{H}\mathbf{R}) = \det(\mathbf{H}) \tag{29}$$

Comparing (28) and (29),we obtain

$$\det(\mathbf{\Lambda})\det(\mathbf{D}) = \det(\mathbf{H}) = \det(\mathbf{U})\det(\mathbf{\Lambda})\det(\mathbf{V}) \tag{30}$$

Because $\det(\mathbf{\Lambda}) = \lambda_1\lambda_2\ldots\lambda_n \geq 0$, *if* $\det(\mathbf{H}) > 0$, $\det(\mathbf{D}) = 1$ *and if* $\det(\mathbf{H}) < 0$, $\det(\mathbf{D}) = -1$.

On the other hand,

$$F(\mathbf{R}) = -tr(\mathbf{RH}) = -tr(\mathbf{HR}) = -tr(\mathbf{L}') \tag{31}$$

Substituting (27) into (31), we have

$$F(\mathbf{R}) = -tr(\mathbf{U\Lambda DU}^T) = -tr(\mathbf{\Lambda D}) = -\sum_{i=1}^{m}\lambda_i d_i \tag{32}$$

Therefore, to get the maximum of F(**R**), *Then, when* $\det(\mathbf{H}) > 0$ *or* $\det(\mathbf{U})\det(\mathbf{V}) = +1$,

$$\begin{cases} d_1 = d_2 = \ldots = d_m = -1, & m \text{ is even} \\ d_1 = d_2 = \ldots = d_{m-1} = -1, d_m = 1, & m \text{ is odd} \end{cases} \tag{33}$$

When $\det(\mathbf{H}) < 0$ *or* $\det(\mathbf{U})\det(\mathbf{V}) = -1$,

$$\begin{cases} d_1 = d_2 = \ldots = d_m = -1, & m \text{ is odd} \\ d_1 = d_2 = \ldots = d_{m-1} = -1, d_m = 1, & m \text{ is even} \end{cases} \tag{34}$$

Finally, substituting $\mathbf{L'}^{-1} = (\mathbf{U\Lambda DU}^T)^{-1} = \mathbf{U\Lambda}^{-1}\mathbf{D}^{-1}\mathbf{U}^T$ *into (24), we obtain*

$$\mathbf{R} = \mathbf{H}^T\mathbf{L'}^{-1} = (\mathbf{V\Lambda U}^T)(\mathbf{U\Lambda}^{-1}\mathbf{D}^{-1}\mathbf{U}^T) = \mathbf{VDU}^T \tag{35}$$

3.3.2. Scale computation

For a given **R**, maximizing $F(s, \mathbf{R})$ is equivalent to maximizing $F(s)$ as following shows.

$$F(s) = \sum_{i=1}^{N_x}\exp\left(-||s\mathbf{R}\vec{p}_i - \vec{q}_i||_2^2/(2\sigma^2)\right) \tag{36}$$

Taking the derivative with respect to s, we get

$$s = \sum_{i=1}^{N_x} F(s)(\mathbf{R}\vec{p}_i)^T\vec{q}_i / \sum_{i=1}^{N_x} F(s)(\mathbf{R}\vec{p}_i)^T\mathbf{R}\vec{p}_i \tag{37}$$

where $F(s)$ can use the scale factor of last step to approximate in iteration.

3.3.3. Translation computation

If rotation and scale transformation are computed, according to (10), we calculate $\vec{t}_k$:

$$\vec{t}_k = \sum_{i=1}^{N_x}(\vec{y}_{c_k(i)} - s_k\mathbf{R}_k\vec{x}_i)w_i / \sum_{i=1}^{N_x} w_i \tag{38}$$

From what is discussed above, the scale, rotation and translation transformations of (8) are all computed. From the whole algorithm, we know that it is similar to the ICP algorithm. Although the points in the data set may not always be able to find the correct corresponding points in the model set, they move to the correct points nearer and nearer in iterations. Hence, the algorithm can reach the best registration finally.

3.4. Convergence analysis

In this section, the convergence of our algorithm will be discussed. As stated before, our algorithm shares the same procedure as the ICP algorithm, where the model shape searches the closest points in the data shape via iteration. It is therefore a locally convergent algorithm, which is formally stated below.

Theorem 1. *The robust scale ICP algorithm based on correntropy converges asymptotically to a local optimum for any given initial parameters.*

Proof. Given two point sets $X \triangleq \{\vec{x}_i\}_{i=1}^{N_x}$ and $Y \triangleq \{\vec{y}_i\}_{i=1}^{N_y}$. In the kth iteration, $\{s_{k-1}, \mathbf{R}_{k-1}, \vec{t}_{k-1}\}$ is known. Let $\vec{x}'_{i,k-1} \triangleq s_{k-1}\mathbf{R}_{k-1}\vec{x}_i + \vec{t}_{k-1}$, and we can compute its corresponding closest point $\vec{y}_{c_k(i)}$ in the data shape. Therefor, we get

$$F_k(s_{k-1}, \mathbf{R}_{k-1}, \vec{t}_{k-1}) = \sum_{i=1}^{N_x}\exp\left(-\frac{\left\|\vec{x}'_{i,k-1} - \vec{y}_{c_k(i)}\right\|_2^2}{2\sigma^2}\right). \tag{39}$$

Because $\{\vec{x}'_i\}$ is to register $\{\vec{y}_{c_k(i)}\}$, we compute the best spatial transformation $\{s_k, \mathbf{R}_k, \vec{t}_k\}$. Hence, the objective function now becomes

$$F_k(s_k, \mathbf{R}_k, \vec{t}_k) = \sum_{i=1}^{N_x}\exp\left(-\frac{\left\|s_k\mathbf{R}_k\vec{x}_i + \vec{t}_k - \vec{m}_{c_k(i)}\right\|_2^2}{2\sigma^2}\right). \tag{40}$$

Because $\{s_k, \mathbf{R}_k, \vec{t}_k\}$ is obtained by maximizing (8), it is obvious that

$$F_k\left(s_{k-1}, \mathbf{R}_{k-1}, \vec{t}_{k-1}\right) \le F_k\left(s_k, \mathbf{R}_k, \vec{t}_k\right) \tag{41}$$

Next, in the $(k+1)$th iteration, suppose

$$\vec{x}'_{i,k} \triangleq s_k\mathbf{R}_k\vec{x}_i + \vec{t}_k$$

and we find its corresponding point $\vec{y}_{c_{k+1}(i)}$ in the data shape, too. Then,

$$F_{k+1}(s_k, \mathbf{R}_k, \vec{t}_k) = \sum_{i=1}^{N_x}\exp\left(-\frac{\left\|\vec{x}'_{i,k} - \vec{y}_{c_{k+1}(i)}\right\|_2^2}{2\sigma^2}\right) \tag{42}$$

For $c_{k+1}(i)$ is obtained by minimizing (7), we know that

$$\begin{aligned} F_k(s_k, \mathbf{R}_k, \vec{t}_k) &= \sum_{i=1}^{N_x}\exp\left(-\frac{\left\|\vec{x}'_{i,k} - \vec{y}_{c_k(i)}\right\|_2^2}{2\sigma^2}\right) \\ &\le \sum_{i=1}^{N_x}\exp\left(-\frac{\left\|\vec{x}'_{i,k} - \vec{y}_{c_{k+1}(i)}\right\|_2^2}{2\sigma^2}\right) = F_{k+1}\left(s_k, \mathbf{R}_k, \vec{t}_k\right) \end{aligned} \tag{43}$$

Because the maximum of the exponential function here is 1, the value of function $F(.)$ will not be larger than N_x. Hence, we can obtain

$$\begin{aligned} &F_1(s_0, \mathbf{R}_0, \vec{t}_0) \le F_1(s_1, \mathbf{R}_1, \vec{t}_1) \le F_2(s_1, \mathbf{R}_1, \vec{t}_1) \le \ldots \\ &\le F_k(s_{k-1}, \mathbf{R}_{k-1}, \vec{t}_{k-1}) \le F_k(s_k, \mathbf{R}_k, \vec{t}_k) \le F_{k+1}(s_k, \mathbf{R}_k, \vec{t}_k) \\ &\le N_x. \end{aligned} \tag{44}$$

Finally, According to the Monotonic Sequence Theorem "Every bounded monotonic sequence of real numbers is convergent", it is proved that our algorithm converges monotonically to a local maximum. □

4. Experimental results

To verify the fast speed and robustness of our presented method, we compare the robust scale ICP algorithm based on correntropy with the traditional scale ICP algorithm and CPD algorithm [35] by experiments on simulation and standard data including the Part B of CE-Shape-1 [36] and the Stanford 3D Scanning Repository [37]. In order to validate the accuracy our algorithm, the errors of the computed transformation and the true transformation on these three algorithms are calculated in the experiments. The average computation times spent on each iteration in these three algorithms are examined. A number of registration results are displayed. The experiments are conducted by MATLAB 2014a and run on PC with AMD A10-5800 K APU 3.8 GHz CPU and 8.0 GB RAM.

4.1. 2D Simulation

In this section, simulation experiments are conducted to compare the registration accuracy of our algorithm with traditional scale ICP algorithm and CPD algorithm. And the simulation process is designed as follows.

First of all, a random scale transformation is generated which is denoted as $\{s_r, \mathbf{R}_r, \vec{t}_r\}$ and we apply it on model point sets to get the data point sets. After that, we add random noises and outliers manually to the data point sets to obtain noisy data point

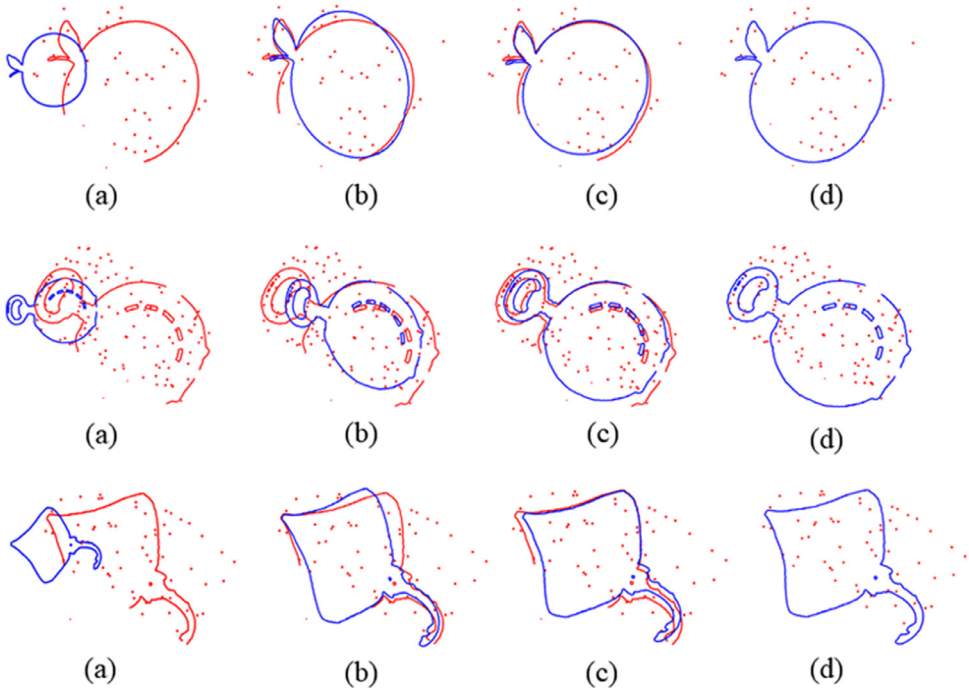

Fig. 2. Registration results of 2D simulated point sets. (a) Point sets before registration. (b) Results of scale ICP. (c) Results of CPD. (d) Results of our algorithm.

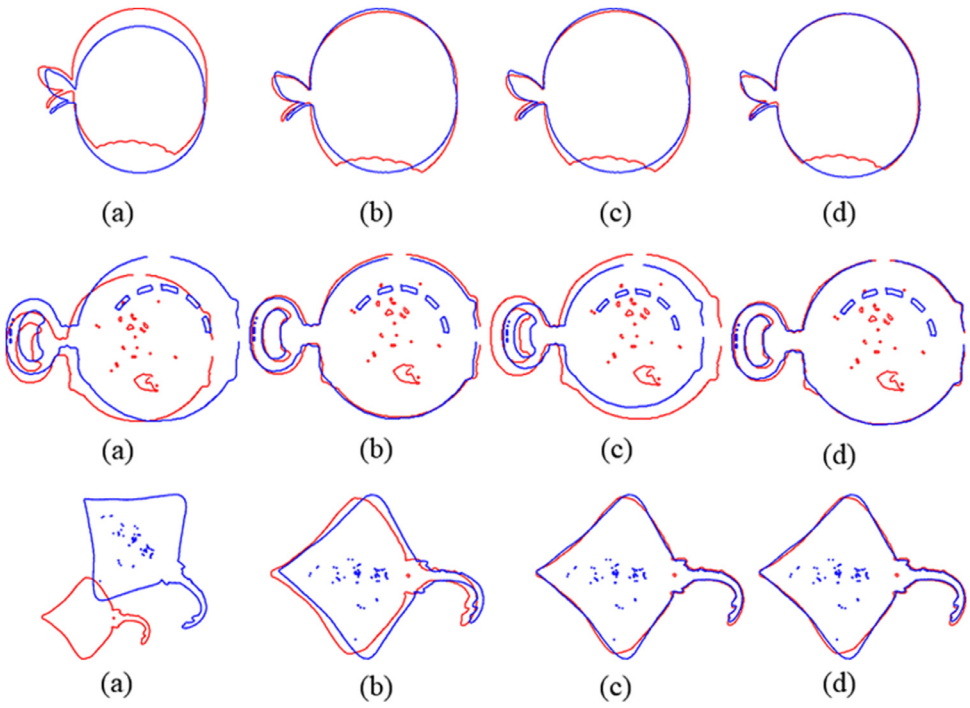

Fig. 3. Registration results of 2D shapes. (a) Point sets before registration. (b) Results of scale ICP. (c) Results of CPD. (d) Results of our algorithm.

sets. Then, the model point sets are registered to corresponding data point sets using scale ICP algorithm, CPD and our algorithm respectively and their computed transformation is denoted as $\{s_{method}, \mathbf{R}_{method}, \vec{t}_{method}\}$.

Actually, the generated random scale transformation is the ground-truth of the scale transformation, that is, $\{s_{true}, \mathbf{R}_{true}, \vec{t}_{true}\} = \{s_r, \mathbf{R}_r, \vec{t}_r\}$. Therefore, To quantify the registration results of three algorithms, their registration errors are defined as $\varepsilon_s = |s_{method} - s_{true}|$, $\varepsilon_{\mathbf{R}} = \|\mathbf{R}_{method} - \mathbf{R}_{true}\|_2$ and $\varepsilon_{\vec{t}} = \left\|\vec{t}_{method} - \vec{t}_{true}\right\|_2$. All compared results are summarized as Table 1. From the table, we can find that our algorithm can get the least errors including ε_s, $\varepsilon_{\mathbf{R}}$ and $\varepsilon_{\vec{t}}$, which demonstrates that our algorithm is robust in scale registration with outliers.

To observe the registration results more intuitively, we display all the results in Fig 2. From the figure, we can get the same conclusion that our algorithm performs much better than the other two algorithms in noisy point set registration.

4.2. 2D Standard database

In the following experiments, both the model point sets and data point sets are acquired from a 2D standard database, the Part

Table 1
Comparison of 2D simulation results.

Data	ε_s			$\varepsilon_{\mathbf{R}}$			$\varepsilon_{\vec{t}}$		
	Scale ICP	CPD	Our algorithm	Scale ICP	CPD	Our algorithm	Scale ICP	CPD	Our algorithm
Apple	0.0687	0.1061	0.0020	0.3031	0.0889	9.0351e-4	80.0321	32.0936	0.0817
Pocket	0.4158	0.1631	0.0017	0.3489	0.0163	8.9064e-4	136.0093	34.8762	0.0182
Ray	0.1170	0.1398	0.0018	0.2397	0.0264	0.0010	59.8777	37.1835	0.1530

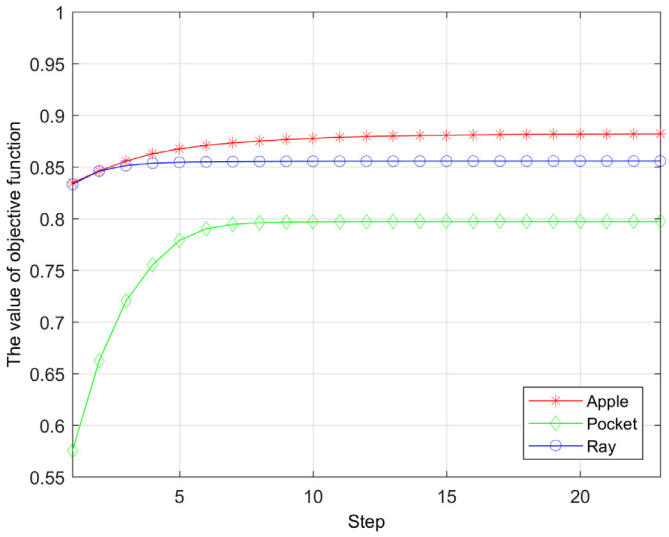

Fig. 4. The convergence of our algorithm.

Table 2
Computation time comparison of 2D point sets (unit: second).

Data	Algorithm		
	Scale ICP	CPD	Our Algorithm
Apple	0.0022	0.0462	0.0083
Pocket	0.0035	0.0632	0.0183
Ray	0.0048	0.0943	0.0329

B of CE-Shape-1. To test the ability to eliminate outliers or noise of scale ICP algorithm, CPD and our algorithm, data point sets with outliers or noise are selected to register to model point sets.

Fig. 3 displays the registration results of Apple, Pocket and Ray. From the results of Ray, we can find that CPD and our algorithm perform well, and both of them reach better registration results than traditional scale ICP. From the results of Apple and Pocket, it can be seen that our algorithm get best results compared to the other two algorithms, which demonstrates that our algorithm has great advantages in the scale registration of noisy point sets.

Moreover, to analyze the speed of three algorithms, the average performance time of each iterative step of scale ICP, CPD and our algorithm is summarized in Table 2. The table shows that our algorithm is slower than scale ICP algorithm for the reason that our algorithm has an exponent calculating. However, our algorithm still has fast speed when comparing with CPD algorithm, which is nearly one-third of it. In addition, Fig. 4 shows the curve of our algorithm's objective function respect to Apple, Pocket and Ray data, which proves that our algorithm is convergent again.

4.3. 3D Simulation

In this section, we will test the performance of our algorithm in 3D point sets. As the number of 3D data points is quite large and CPD algorithm is time consuming, we only compare our algorithm with traditional scale ICP algorithm here.

Similar to 2D point set registration, we conduct the simulation first. The model point set was selected from the Stanford 3D Scanning Repository, and we get the data point sets by applying a random scale transformation and adding random noise or outliers to model point sets. Then, the registration errors can be obtained, which is shown in Table 3.

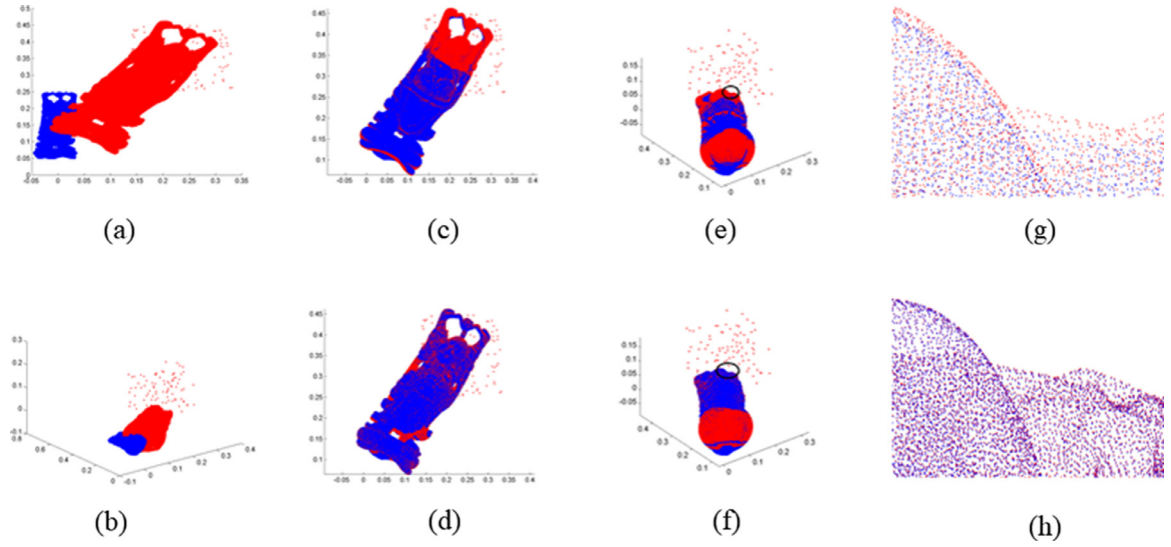

Fig. 5. Registration results of 3D simulation on Happy data. (a) 2D view of point sets before registration. (b) 3D view of point sets before registration. (c) 2D view of scale ICP's registration results. (d) 2D view of our algorithm's registration results. (e) 3D view of scale ICP's registration results. (f) 3D view of our algorithm's registration results. (g) Local amplification of scale ICP's results. (h) Local amplification of our algorithm's results.

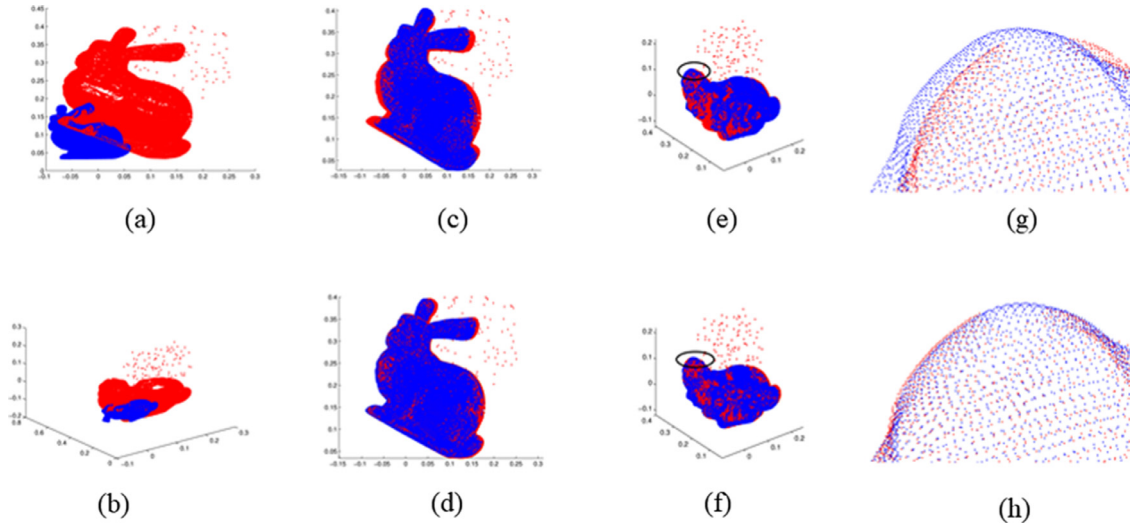

Fig. 6. Registration results of 3D simulation on Bunny data. (a) 2D view of point sets before registration. (b) 3D view of point sets before registration. (c) 2D view of scale ICP's registration results. (d) 2D view of our algorithm's registration results. (e) 3D view of scale ICP's registration results. (f) 3D view of our algorithm's registration results. (g) Local amplification of scale ICP's results. (h) Local amplification of our algorithm's results.

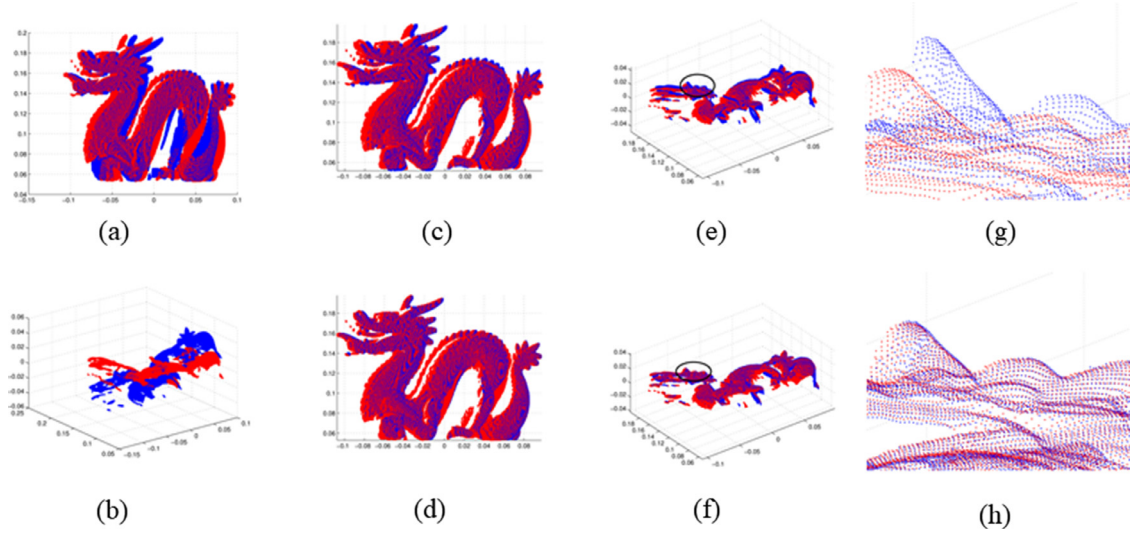

Fig. 7. Registration results of 3D database on Dragon data. (a) 2D view of point sets before registration. (b) 3D view of point sets before registration. (c) 2D view of scale ICP's registration results. (d) 2D view of our algorithm's registration results. (e) 3D view of scale ICP's registration results. (f) 3D view of our algorithm's registration results. (g) Local amplification of scale ICP's results. (h) Local amplification of our algorithm's results.

Table 3
Comparison of 3D simulation results.

Data	ε_s		$\varepsilon_{\mathbf{R}}$		$\varepsilon_{\vec{t}}$	
	Scale ICP	Our algorithm	Scale ICP	Our algorithm	Scale ICP	Our algorithm
Happy	0.0114	0.0040	0.0145	0.0035	0.0058	2.7505e-4
Bunny	0.0314	0.0159	0.1265	0.0398	0.0165	0.0042
Dragon	0.0290	0.0063	0.1213	0.0035	0.0196	6.8352e-5

From Table 3, we can see that our algorithm has smaller errors including scale factor, rotation and translation than traditional scale ICP algorithm which demonstrates our algorithm's high accuracy in noisy point set registration.

In addition, we can observe the registration effect intuitively from the results displayed in Figs. 5 and 6. Figs. 5 and 6 display the simulation results of Happy and Bunny data respectively. In the figures, (a) and (b) is 2D view and 3D view of point sets waiting for registration, in which including a scale transformation. Moreover, (c) and (d) is 2D view of these two algorithms while (e) and (f) is 3D view of them. It seems that both two algorithms perform well in scale registration. However, when we amplify the local areas marked in (e) and (f), which is shown in (g) and (h) respectively, we can find that the results of our algorithm are better than scale ICP especially from the margin.

4.4. 3D standard database

Different with the simulation, both the model point sets and data point sets in the following experiments are chose from Stan-

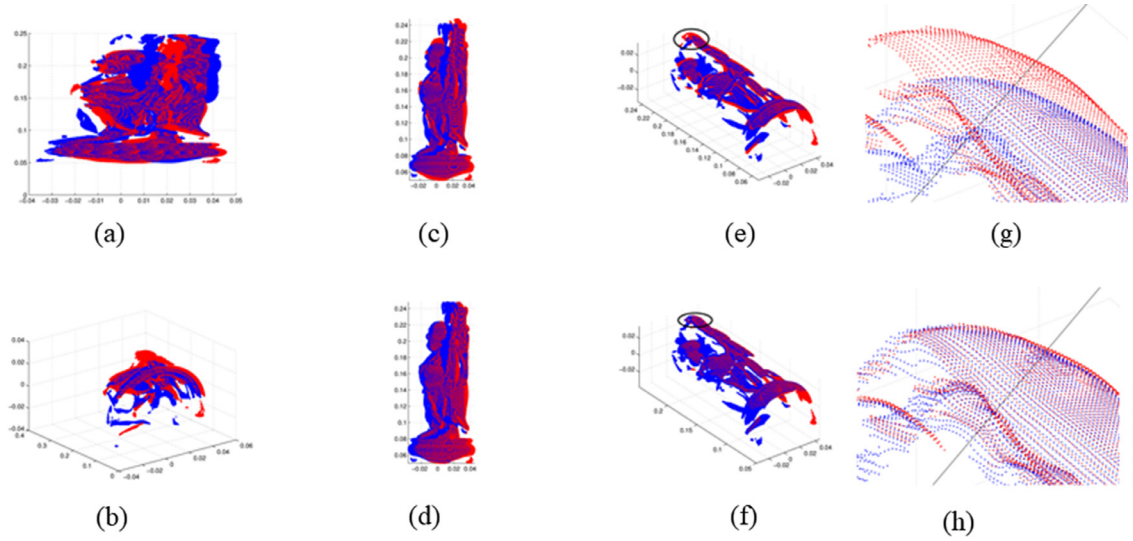

Fig. 8. Registration results of 3D database on Happy data. (a) 2D view of point sets before registration. (b) 3D view of point sets before registration. (c) 2D view of scale ICP's registration results. (d) 2D view of our algorithm's registration results. (e) 3D view of scale ICP's registration results. (f) 3D view of our algorithm's registration results. (g) Local amplification of scale ICP's results. (h) Local amplification of our algorithm's results.

ford 3D Scanning Repository, a standard 3D database. Two examples containing Dragon and Happy data are shown here to observe the registration effect of scale ICP algorithm and our algorithm.

Fig. 7 displays the results of Dragon data. Because the model point set can't match data point set exactly, traditional scale ICP algorithm is affected by the outliers or noise and performs badly. However, correntropy is local which means that its value is primarily decided by the most similar point-pairs while the value of noisy points is too small to be ignored. Therefore, we can see that our algorithm gets better results from the local amplification as Fig. 7(g) and 7(h) shown.

More examples are displayed in Fig. 8. For the similarity measure MSE is global which means that all the points of the model shape will contribute equal to the value of similarity measure, so the results of the scale ICP algorithm are worse because of the noisy points as Fig. 8(g) shown. And Fig. 8(h) shows that our algorithm registers well regardless of the interference of noise.

5. Conclusions

This paper proposes a robust scale ICP algorithm based on correntropy for scale registration between two m-D point sets with large noises and outliers. By making a comparison between correntropy and MSE, it is obvious that correntropy has the capacity to eliminate the interference of noise or outliers and is more suitable to deal with registration problem with noisy point sets. Hence, we introduce correntropy as the similarity measure to build a new objective function for scale registration. To solve the objective function, the half-quadratic method is used to derive a robust scale ICP algorithm. The closed-form solution of the algorithm is given in each iteration. Similar to the traditional scale ICP algorithm, the algorithm proposed shares the same process. At each iterative step, it finds the closest points based on the current scale transformation to establish index matching firstly, and then computes the new scale transformation based on the known index matching. Besides, it is proved that our algorithm converges to a local maximum monotonically in theory. Experiment results of 2D and 3D registration proved that our algorithm can successfully estimate rotation, translation and scale factor between roughly pre-aligned point sets. And these experiments demonstrate that our algorithm is more accurate and has fast speed in noisy point set registration in contrast to traditional scale ICP algorithm and CPD algorithm.

Although the robust scale ICP algorithm improves the accuracy and speed of scale registration, there are still a lot of other problems needed to be solved. For example, selecting a proper initial value to make the algorithm get global optimal solutions or controlling the kernel bandwidth to obtain higher accuracy.

Acknowledgment

This work was supported by the National Natural Science Foundation of China under Grant Nos. 61673126, 61573274, U1701261 and 61627811.

References

[1] A. Goshtasby, Piecewise linear mapping functions for image registration, Pattern Recognit. 19 (6) (1986) 459–466.
[2] C. Studholme, D.L. Hill, D.J. Hawkes, An overlap invariant entropy measure of 3d medical image alignment, Pattern Recognit. 32 (1) (1999) 71–86.
[3] H. Lester, S.R. Arridge, A survey of hierarchical non-linear medical image registration, Pattern Recognit. 32 (1) (1999) 129–149.
[4] S. Du, Y. Guo, G. Sanroma, D. Ni, G. Wu, D. Shen, Building dynamic population graph for accurate correspondence detection, Med. Image Anal. 26 (1) (2015) 256–267.
[5] P.J. Besl, N.D. McKay, A method for registration of 3D shapes, IEEE Trans. Pattern Anal. Mach. Intell. 14 (2) (1992) 239–256.
[6] Y. Chen, G. Medioni, Object modelling by registration of multiple range images, Image Vis. Comput. 10 (3) (1992) 145–155.
[7] Z. Zhang, Iterative point matching for registration of free-form curves and surfaces, Int. J. Comput. Vis. 13 (2) (1994) 119–152.
[8] H. Zha, M. Ikuta, T. Hasegawa, Registration of range images with different scanning resolutions, in: Proceedings of the IEEE International Conference on Systems, Man, and Cybernetics, 2, 2000, pp. 1495–1500.
[9] S. Ying, J. Peng, S. Du, H. Qiao, A scale stretch method based on ICP for 3D data registration, IEEE Trans. Autom. Sci. Eng. 6 (3) (2009) 559–565.
[10] G. Dalley, P. Flynn, Pair-wise range image registration: a study in outlier classification, Comput. Vis. Image Understand. 87 (1) (2002) 104–115.
[11] T. Zinßer, J. Schmidt, H. Niemann, Point set registration with integrated scale estimation, in: Proceedings of the Eighth International Conference on Pattern Recognition and Image Processing, 116, 2005, p. 119.
[12] H. Zhang, O. Hall-Holt, A. Kaufman, Range image registration via probability field, in: Proceedings of the Computer Graphics International, IEEE, 2004, pp. 546–552.
[13] B. Jensen, R. Siegwart, Scan alignment with probabilistic distance metric, in: Proceedings of the IEEE/RSJ International Conference on Intelligent Robots and Systems(IROS), 3, 2004, pp. 2191–2196.
[14] S. Du, J. Liu, C. Zhang, J. Zhu, K. Li, Probability iterative closest point algorithm for M-D point set registration with noise, Neurocomputing 157 (2015) 187–198.

[15] S. Du, J. Liu, B. Bi, J. Zhu, J. Xue, New iterative closest point algorithm for isotropic scaling registration of point sets with noise, J. Vis. Commun. Image Represent 38 (2016) 207–216.
[16] D. Rodriguez-Losada, J. Minguez, Improved data association for ICP-based scan matching in noisy and dynamic environments, in: Proceedings of the IEEE International Conference on Robotics and Automation, 2007, pp. 3161–3166.
[17] Y. Liu, M.A. Rodrigues, Accurate registration of structured data using two overlapping range images, in: Proceedings of the IEEE International Conference on Robotics and Automatio (ICRA), 3, 2002, pp. 2519–2524.
[18] S. Rusinkiewicz, M. Levoy, Efficient variants of the ICP algorithm, in: Proceedings of the Third International Conference on 3-D Digital Imaging and Modeling (3DIM), IEEE, 2001, pp. 145–152.
[19] N. Gelfand, L. Ikemoto, S. Rusinkiewicz, M. Levoy, Geometrically stable sampling for the ICP algorithm, in: Proceedings of the Fourth International Conference on 3-D Digital Imaging and Modeling(3DIM), IEEE, 2003, pp. 260–267.
[20] W. Liu, P.P. Pokharel, J.C. Príncipe, Correntropy: properties and applications in non-gaussian signal processing, IEEE Trans. Signal Process. 55 (11) (2007) 5286–5298.
[21] R. He, W.-S. Zheng, B.-G. Hu, X.-W. Kong, A regularized correntropy framework for robust pattern recognition, Neural Comput. 23 (8) (2011) 2074–2100.
[22] R. He, T. Tan, L. Wang, W.-S. Zheng, l 2, 1 regularized correntropy for robust feature selection, in: Proceedings of the Conference on Computer Vision and Pattern Recognition (CVPR), IEEE, 2012, pp. 2504–2511.
[23] Z. Wu, S. Peng, B. Chen, H. Zhao, Robust hammerstein adaptive filtering under maximum correntropy criterion, Entropy 17 (10) (2015) 7149–7166.
[24] R. He, B.-G. Hu, W.-S. Zheng, X.-W. Kong, Robust principal component analysis based on maximum correntropy criterion, IEEE Trans. Image Process. 20 (6) (2011) 1485–1494.
[25] R. He, W.-S. Zheng, B.-G. Hu, Maximum correntropy criterion for robust face recognition, Trans. Pattern Anal. Mach. Intell. 33 (8) (2011) 1561–1576.
[26] B. Chen, L. Xing, J. Liang, N. Zheng, J.C. Principe, Steady-state mean-square error analysis for adaptive filtering under the maximum correntropy criterion, IEEE Signal Process Lett. 21 (7) (2014) 880–884.
[27] B. Chen, L. Xing, H. Zhao, N. Zheng, J.C. Príncipe, Generalized correntropy for robust adaptive filtering, IEEE Trans. Signal Process. 13 (64) (2015) 3376–3387.
[28] B. Chen, J. Wang, H. Zhao, N. Zheng, J.C. Príncipe, Convergence of a fixed-point algorithm under maximum correntropy criterion, IEEE Signal Process Lett. 22 (10) (2015) 1723–1727.
[29] M. Greenspan, M. Yurick, Approximate KD tree search for efficient ICP, in: Proceedings of the Fourth International Conference on 3-D Digital Imaging and Modeling (3DIM), IEEE, 2003, pp. 442–448.
[30] C.B. Barber, D.P. Dobkin, H. Huhdanpaa, The Quickhull algorithm for convex hulls, ACM Trans. Math. Softw. (TOMS) 22 (4) (1996) 469–483.
[31] R. Dahyot, P. Charbonnier, F. Heitz, Robust visual recognition of colour images, in: Proceedings of the Conference on Computer Vision and Pattern Recognition, 1, IEEE, 2000, pp. 685–690.
[32] X.-T. Yuan, B.-G. Hu, Robust feature extraction via information theoretic learning, in: Proceedings of the 26th annual international conference on machine learning, ACM, 2009, pp. 1193–1200.
[33] R. He, B.-G. Hu, W.-S. Zheng, Y. Guo, et al., Two-stage sparse representation for robust recognition on large-scale database, in: Proceedings of the AAAI, 10, 2010, p. 1.
[34] R.T. Rockafellar, Convex Analysis, Princeton University Press, 2015.
[35] A. Myronenko, X. Song, Point set registration: coherent point drift, IEEE Trans. Pattern Anal. Mach. Intell. 32 (12) (2010) 2262–2275.
[36] L.J. Latecki, R. Lakamper, T. Eckhardt, Shape descriptors for non-rigid shapes with a single closed contour, in: Proceedings of the IEEE Conference on Computer Vision and Pattern Recognition, 1, 2000, pp. 424–429.
[37] M. Levoy, J. Gerth, B. Curless, K. Pull, The stanford 3D scanning repository, http://www-graphics.stanford.edu/data/3dscanrep (2005).

Zongze Wu received the B.S. degree in material forming and control, the M.S. degree in control science and engineering, and the Ph.D. degree in pattern reorganization and intelligence system, all from Xi'an Jiaotong University, Xi'an, China, in 1999, 2002, and 2005, respectively. He is currently a Professor in the School of Automation, Guangdong University of Technology, Guangzhou, China. His research interests include pattern recognition, Artificial intelligence and Intelligent manufacturing. Dr. Wu received the Microsoft Fellowship Award of the MSRA in 2003. He got a first prize of Ministry of Education technological innovation in 207. He won the Technological Award first prize of Guangdong Province four times in 2008, 2013, 2014, 2018, respectively. He got a second prize of Ministry of Education technological innovation twice, in 2012 and 2013.

Hongchen Chen received Bachelor degree in electronic information engineering from Xidian University, China in 2016. He is currently pursuing his ph.D in the school of electronic and information in South China University of Technology. His research interests include image registration, CMOS millimeter-wave intergrated circuits and low noise amplifier design.

Shaoyi Du received B.S. degrees both in computational mathematics and in computer science, M.S. degree in applied mathematics and Ph.D. degree in pattern recognition and intelligence system from Xi'an Jiaotong University, China in 2002, 2005 and 2009 respectively. He worked as a postdoctoral fellow in Xi'an Jiaotong University from 2009 to 2011 and visited University of North Carolina at Chapel Hill from 2013 to 2014. He is currently a professor of the Institute of Artificial Intelligence and Robotics in Xi'an Jiaotong University. His research interests include image registration, mobile robot, object detection and recognition.

Minyue Fu received the Bachelor degree in electrical engineering from the University of Science and Technology of China, Hefei, China, in 1982, and M.S. and Ph.D. degrees in electrical engineering from the University of Wisconsin-Madison in 1983 and 1987, respectively. From 1987 to 1989, he served as an Assistant Professor in the Department of Electrical and Computer Engineering, Wayne State University, Detroit, MI. He joined the Department of Electrical and Computer Engineering, the University of Newcastle, Callaghan, NSW, Australia, in 1989. Currently, he is a Chair Professor in Elec-trical Engineering. He was a Visiting Associate Professor at University of Iowa in 1995996, a Senior Fellow/Visiting Professor at Nanyang Technological University, Singapore, in 2002, and a Visiting Professor at Tokyo University in 2003. He has held a ChangJiang Visiting Professorship at Shandong University, a visiting Professorship at South China University of Technology, and a Qian-ren Professorship at Zhejiang University in China. His main research interests include control systems, signal processing, and communications. His current research projects include networked control systems, smart electricity networks, and super-precision positioning control systems. Dr. Fu was an Associate Editor for the IEEE TRANSACTIONS ON AUTO-MATIC CONTROL, Automatica, IEEE TRANSACTIONS ON SIGNAL PROCESS-ING,and the Journal of Optimization and Engineering.

Nan Zhou is a Ph.D. student in the School of Automation Engineering, University of Electronic Science and Technology of China, Chengdu, Sichuan. He is jointly supervised by Department of Electrical and Computer Engineering, University of Alberta. His research interests include sparse modelling, machine learning, feature selection, and sparse modeling.

Nanning Zheng graduated from the Department of Electrical Engineering, Xi'an Jiaotong University, Xi'an, China, in 1975, and received the M.S. degree in information and control engineering from Xi'an Jiaotong University in 1981 and the Ph.D. degree in electrical engineering from Keio University, Yokohama, Japan, in 1985. He jointed Xi'an Jiaotong University in 1975, and he is currently a Professor and the Director of the Institute of Artificial Intelligence and Robotics, Xi'an Jiaotong University. Since August 2003, he has been the President of Xi'an Jiaotong University. His research interests include computer vision, pattern recognition, machine vision and image processing, neural networks, and hardware implementation of intelli-

gent systems. Dr. Zheng became a member of the Chinese Academy of Engineering in 1999 and has been the chief scientist and the director of the Information Technology Committee of the China National High Technology Research and Development Program since 2001. He was General Chair of the International Symposium on Information Theory and Its Applications and General Co-Chair of the International Symposium on Nonlinear Theory and Its Applications, both in 2002. He is a member of the Board of Governors of the IEEE ITS Society and the Chinese Representative on the Governing Board of the International Association for Pattern Recognition. He also serves as an executive deputy editor of the Chinese Science Bulletin. He is now an IEEE fellow.